High performance organic-inorganic hybrid barrier coating for encapsulation of OLEDs†

KyungHo Jung,[a] Jun-Young Bae,[a] Soo Jin Park,[b] Seunghyup Yoo[b] and Byeong-Soo Bae*[a]

Received 24th June 2010, Accepted 21st October 2010
DOI: 10.1039/c0jm02008g

UV curable cycloaliphatic epoxy functionalized oligosiloxane resin is synthesized by non-hydrolytic sol–gel reaction for application in encapsulation of organic light emitting devices (OLEDs). The physical and chemical properties of polymerized cycloaliphatic epoxy hybrid materials (hybrimers) are easily tunable by controlling the precursors. A single hybrimer coating on a PET film is optically transparent and shows low permeability of up to 0.68 g m^{-2} day^{-1} per mil measured by a Ca degradation test. It is found that the permeability is influenced by the siloxane and epoxy network density, and the surface energy of the coating. An optimized hybrimer barrier coated film is applied to the encapsulation of an OLED with the aim of extending life-time.

Introduction

High performance transparent gas barrier coating materials have attracted much attention in conjunction with the use of plastic substrates enable the fabrication of the flexible displays, solar cells, and opto-devices due to their high flexibility, thermal stability, and optical transparency.[1–3] OLEDs are promising candidates for next generation displays. However, their organic functional layers have high sensitivity to water and oxygen.[4,5] Desired encapsulation materials must therefore not only prevent infiltration of oxygen and water molecules into OLED devices, but should also be transparent in the visible region. Polymer substrates also have limitations such as high permeability to gases, water vapor and volatile organic compounds that restrict their application. To meet the requirements of impermeability, inorganic thin films that have excellent barrier properties have been widely used as OLED barrier coatings.[6,7] However, when deposited on flexible substrates, many defects are formed, such as pinholes and cracks, which can act as oxygen and water molecule propagation channels. Consequently, to suppress crack generation, polymer and inorganic composite multi-layers (dyads) have been used as high performance gas barrier films.[8,9] The fabrication process, however, is too complicated. In addition, vacuum processes, which require expensive equipment and thus result in high fabrication costs, are required.

Given this background, new and versatile materials with low permeation to oxygen and water molecules are needed for application to organic electronics. Organic-inorganic hybrid materials, synthesized by hydrolytic sol–gel reaction, have recently been introduced.[10,11] It has been reported that organic-inorganic hybrid materials show higher barrier properties for water vapor and oxygen than commercially available polymers, because they contain UV and/or thermally polymerizable organic functional groups and highly condensed inorganic networks. These organic-inorganic hybrid materials may minimize the amount of packing materials and also reduce the number of dyads. However, typical WVTR values achieved thus far are 4 and 20 g m^{-2} day^{-1} per 1 mil (25 μm).[11] Non-hydrolytic sol–gel derived siloxane based organic–inorganic hybrid materials (hybrimers), wherein inorganic networks such as siloxane bonds can form by a simple condensation reaction without water, have been widely studied for many applications.[12–15] With a suitable selection of precursors and optimization of processing parameters, the organic moieties, condensation degree, surface energy and molecular structure of oligosiloxane can be controlled. In addition, these materials show high thermal and chemical stability due to the existence of siloxane bonds, and high shelf stability due to the absence of water molecules and hydroxyl groups.

In this study, we report a new type of cycloaliphatic epoxy hybrimers produced by UV induced polymerization of sol–gel synthesized cycloaliphatic epoxy oligosiloxane resins to be used as high performance barrier coating materials. For optimization of the synthesis process and barrier properties, we controlled the composition of the precursors. The permeability values (WVTR) of optimized hybrimer barrier coated films were measured by using the Ca degradation method.[16,17] Finally, we demonstrate extended life-time of OLEDs encapsulated with the fabricated hybrimer barrier coated film under harsh conditions.

Scheme 1 chemically illustrates the synthesis of cycloaliphatic epoxy oligosiloxanes by sol–gel condensation of 2-(3,4-epoxycyclohexyl)ethyl-trimethoxysilane (ECTS) and diphenylsilanediol (DPSD), and the fabrication of cycloaliphatic epoxy hybrimers by UV-induced polymerization of the cycloaliphatic epoxy oligosiloxanes with a cationic photo-initiator. In the sol–gel condensation step, hydroxyl groups in DPSD and alkoxy groups in ECTS are directly condensed to form siloxane bonds without using water. Gas barrier materials with a low WVTR must have a highly dense structure, chemically reactive sites to water molecules, and low surface energy. Thus, we optimized the

[a]*Laboratory of Optical Materials and Coating (LOMC), Department of Materials Science and Engineering, KAIST, Daejeon, 305-701, Republic of Korea. E-mail: bsbae@kaist.ac.kr; Fax: +82 42 350 3310; Tel: +82 42 350 4119*
[b]*Integrated Organic Electronics Laboratory (IOEL), Department of Electrical Engineering, KAIST, Daejeon, 305-350, Republic of Korea. E-mail: syoo_ee@kaist.ac.kr; Fax: +82 42 350 8083; Tel: +82 42 350 3483*
† Electronic supplementary information (ESI) available: Supplementary information. See DOI: 10.1039/c0jm02008g

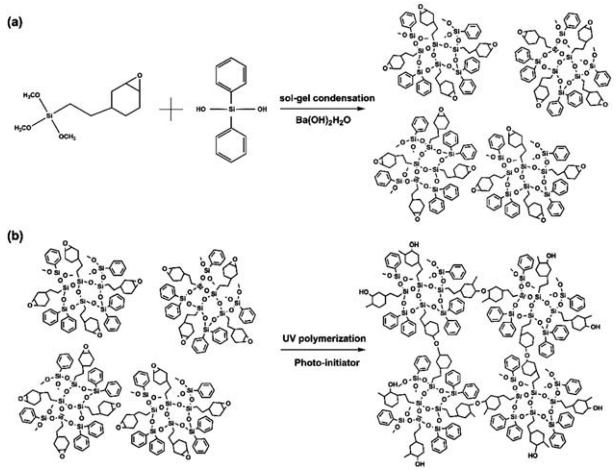

Scheme 1 Schematic diagram of (a) the synthesis of the cycloaliphatic epoxy oligosiloxanes by a sol–gel condensation of ECTS and DPSD and (b) fabrication of hybrimers by UV-induced polymerization of the cycloaliphatic epoxy oligosiloxanes with cationic photo-initiator.

composition of the precursors to achieve a lower water permeability of the hybrimers with high transparency.

Experimental

Synthesis and characterization cycloaliphatic epoxy oligosiloxane resins

We synthesized cycloaliphatic epoxy oligosiloxane resin using a method described in a previous article.[13] ED60 was synthesized by a simple sol–gel condensation reaction between 0.04 mol of ECTS (Gelest, USA) and 0.06 mol of DPSD (Gelest, USA) at 80 °C for 4 h under N_2 purging. Barium hydroxide monohydrate ($Ba(OH)_2H_2O$, 98%, Aldrich, USA) was added as a catalyst to promote the reaction.

^{29}Si nuclear magnetic resonance (NMR, Bruker, USA) spectra of the resin in chloroform-d were recorded using a Bruker FT 500 MHz instrument. The sample temperature was 300 K and the pulse delays were set to 30 s. Fourier transform infrared (FTIR, JASCO, USA) spectra of the cycloaliphatic epoxy oligosiloxanes before and after polymerization were obtained with a resolution of 4 cm^{-1} in a wavenumber ranging from 400 to 4000 cm^{-1}. The distribution of molecular species in the cycloaliphatic epoxy oligosiloxane was examined by matrix-assisted laser desorption and ionization time-of-flight mass spectrometry (MALDI-TOF MS, PerSeptive Biosystems, USA). The spectra of MALDI-TOF MS were obtained with a Voyager-DE STR 4700 proteomics analyzer equipped with a nitrogen laser using a wavelength of 337 nm and a pulse width of 3 ns.

Fabrication and characterization of hybrimer barrier coated film

To fabricate the hybrimer barrier coating film, a poly(ethylene terephthalate) (PET, 100μm) film was carefully cleaned using an ultra-sonicator for 20 min, and then dried in a vacuum oven at 80 °C, for 24 h. To control the viscosity and thickness of the coated film layer, a predetermined amount of solvent, polyethylene glycol methyl ether acetate (PGMEA, Aldrich, USA), was added to the cycloaliphatic epoxy resins. Arylsulfonium hexafluorophosphate salt (Aldrich, USA) was added as a cationic initiator for the photoreaction of cycloaliphatic-epoxy *via* UV light exposure. The typical amount of photo-initiator was 2 wt % of the total weight percent of epoxy-functional groups in the oligosiloxane resin. Subsequently, the diluted cycloaliphatic epoxy oligosiloxane solution with 100 wt% PGMEA was spin-coated at 5000 rpm for 30 s to produce a 2 μm thick layer on the dried PET film. The coated film was photo-polymerized with a mercury UV lamp (λ = 350–390 nm, optical power density = 85 mW cm^{-2}) for 3 min under an air atmosphere. To remove the remaining solvent and promote polymerization, heat treatment at 80 °C for 2 h was applied under a vacuum atmosphere.

The refractive index of the hybrimer barrier coating was obtained using a prism coupler (2010, Metricon, USA) at a wavelength of 632.8 nm. The optical transmittance of the hybrimer coated films was measured using a UV/VIS/NIR spectrophotometer (Shimadzu-3103 PC, Japan). We measured the contact angle (CA) (s-eo 150, Korea) of the hybrimer barrier coated films to calculate the surface energy based on the Owens–Wendt equation.[18] We measured the CA of de-ionized (DI) water and diiodomethane (CH_2I_2, Aldrich, USA) more than 10 times in each sample to minimize the effects of the environmental conditions. A cross sectional image and the surface roughness of the hybrimer coatings were measured by field-emission scanning electron microscopy (FE-SEM, Philips, XL30SFEG, USA) and atomic force microscopy (AFM, Park Science Instrument, Autoprobe 5M, USA). We measured the surface roughness of the hybrimer barrier coating at 5 different points.

Measurement of moisture barrier property

For measuring the permeability of the hybrimer barrier coated films, we used the Ca degradation method.[16,17] Advantages of the Ca degradation method for water vapor and oxygen permeation measurement system include high sensitivity and suitability for oxygen and water vapor permeation studies, good spatial/time resolution, the provision of permeability and diffusivity of the test samples, and flexibility in designing the instrumentation with automatic computerized measurement. First, an Al electrode of 100 nm thickness and a center Ca layer (1.5 × 1.5 cm^2, 250 nm high) were deposited on a carefully cleaned glass substrate through a shadow mask by an e-beam and thermal evaporation system, respectively. The barrier coating and Ca test substrate were sealed with Surlyn (Solaronix SA, Swiss) under pressure at 80 °C. A UV curable epoxy sealant was dispensed on the edge of the test plastic lid to prevent leakage through the side walls. All processes were carried out in a glove box system in ambient nitrogen. We used a PET (2 × 2 cm^2 and 100 μm thick) film as a plate for deposition of the hybrimer barrier coating layers. To calculate the permeability of the hybrimer barrier coating to water vapor, we measured the resistivity change during Ca corrosion at 90% relative humidity (RH), 25 °C. Assuming homogeneous corrosion of the Ca layer from the surface, the resistance R is inversely proportional to height h of the remaining metallic calcium, because oxidized Ca salts are insulators.

$$R = \frac{\rho \times l}{b \times h}$$

where ρ denotes the Ca resistivity and l is the length and b is the width of the Ca layer. The permeation rate P through the barrier coating layer is proportional to the slope of the conductance curve $1/R$, plotted *versus* measurement time t

$$P = -n\,\frac{M(reagent)}{M(Ca)}\,\partial p\,\frac{l}{b}\,\frac{d(1/R)}{dt}$$

where n is the molar equivalent of the degradation reaction, M (reagent) and M (Ca) are the molar masses of the permeating reagent and Ca, respectively, and δ is the density of Ca.

Life time of encapsulated OLEDs

We have fabricated OLED devices on plasma-treated ITO glass substrates in a standard bottom-emitting structure based on 50 nm thick *N*,*N*′-Bis(naphthalen-1-yl)-*N*,*N*′-bis(phenyl)-benzidine (NPB) as a hole transporting layer, 50 nm thick Tris(8-hydroxyquinolinato) aluminium (Alq3) as an emitting and electron transporting layer, and LiF/Al as a cathode. We fabricated the encapsulated OLEDs with a hybrimer barrier coated film using the same method as employed for fabrication of the Ca test sample. All processes were performed in a glove box. To calculate the life-time of the encapsulated OLEDs with the hybrimer barrier coated film, the electrical and emission characteristics of the fabricated devices were determined with a source measurement unit (Keithley 238, USA) and a luminance meter (FDS100-CAL, Thorlab, USA) at 25 °C and 90%RH.

Results and discussion

Characteristics of cycloaliphatic epoxy oligosiloxane resins

Cycloaliphatic epoxy oligosiloxane resins of various compositions were synthesized by non-hydrolytic sol–gel reaction resulting in UV curable, storage stable resins. The precursor composition of different cycloaliphatic epoxy oligosiloxanes are presented in Table 1, where either the degree of condensation of the inorganic network or the molecular weight of oligosiloxane was varied.

The molecular structure of the cycloaliphatic epoxy oligosiloxane resin was characterized by ^{29}Si NMR and FT-IR spectroscopy. Fig. 1 shows ^{29}Si NMR spectra of the cycloaliphatic epoxy oligosiloxane resins with various compositions. In NMR notation, for D^n and T^n, the superscript "n" denotes the number of bridging oxygen atoms to a Si atom. As show in Fig. 1, D^2, T^2, and T^3 peaks are enhanced as the DPSD content in the reactants increases.[12,13] Also, small amounts of unreacted Si species (D^0: 22.9 and 23.4 ppm), which are not desirable for the synthesis of oligosiloxanes, are detected and T^1 peak is almost diminished in ED60 oligosiloxane composition. It means that ED60 oligosiloxane has a more condensed structure as compared to ED40

Table 1 Compositions of silane precursors for synthesis of cycloaliphatic epoxy oligosiloxanes

Composition	ECTS/mol	DPSD/mol	$Ba(OH)_2H_2O$/mol
ED40	0.060	0.040	0.0001
ED50	0.050	0.050	0.0001
ED60	0.040	0.060	0.0001

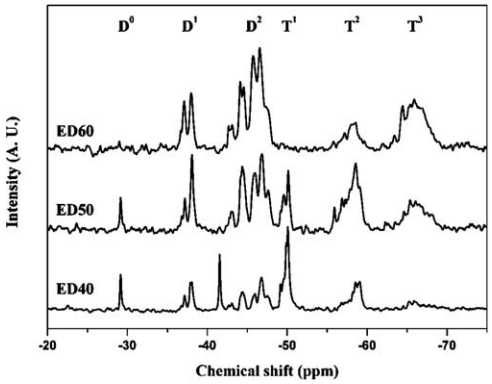

Fig. 1 The ^{29}Si NMR spectra of the cycloaliphatic epoxy oligosiloxane resins synthesized by sol–gel condensation of different compositions of ECTS and DPSD.

oligosiloxane. Theoretically, T^3 species are not formed in the condensation reaction due to the diol radical in the reactants. However, the T^3 peak is present in the spectra. This might be due to a re-esterification reaction of the methoxy group in the ECTS. Water, which is a by-product of the condensation reaction between diol and methanol, produces T^2-OH by hydrolysis of the methoxy group in ECTS. Thus, the self-condensation reaction of T^2-OH species can form T^3 species. Consequently, the degree of condensation (DOC) depending on the DPSD content in the reactants can be calculated using the following equation:[19]

$$DOC = \frac{D^1 + 2D^2 + T^1 + 2T^2 + 3T^3}{2\left(D^0 + D^1 + D^2\right) + 3\left(T^0 + T^1 + T^2 + T^3\right)} \times 100$$

It is found that the DOC increases from about 62.2 to 91.7% as the DPSD content is raised from 40 to 60%.

In the FT-IR spectra (Fig. 2a), Si–O stretching vibrations are observed at 1025 cm^{-1}, and Si–O–Si groups are observed at 1075 cm^{-1} for asymmetric bonds and 1115 cm^{-1} for the cage structure.[20]

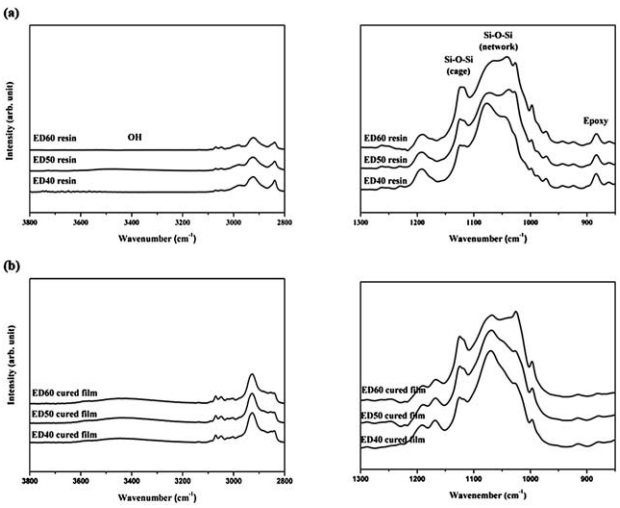

Fig. 2 FT-IR spectra of (a) the cycloaliphatic epoxy oligosiloxane resins synthesized by non-hydrolytic sol–gel condensation of different compositions of ECTS and DPSD, and (b) the cured films.

Peaks of the Si–O–Si asymmetric stretching mode appear at 1110 and 1065 cm^{-1} in the cycloaliphatic epoxy oligosiloxane resins. The cycloaliphatic epoxy group of ECTS, the main compound comprising the resin, is expected to form an organic network in the hybrimer barrier coated film. With an increase in DPSD content, the peak of the Si–O–Si stretching mode increases. This indicates that ED60 oligosiloxane consists of more condensed molecules as compared to ED40 oligosiloxane. Under an acid or base condition, it is necessary to consider the possibility of ring-opening reactions of epoxy groups. Bands due to the vibration of the epoxy groups are observed at 880 cm^{-1}. Peaks of OH groups, which are generated by ring-opening of epoxy groups, are not found in all the spectra. After UV-induced polymerization of the cycloaliphatic epoxy groups in the oligosiloxane resin, bands due to the vibration of the OH groups, which are chemically reactive to water molecules, are observed (Fig. 2 b). Also, there were only small amounts of silanol groups and un-reacted precursors, thereby preventing further self-condensation of the resin. This indicates that the cycloaliphatic epoxy oligosiloxane was well synthesized by a direct condensation reaction between DPSD and ECTS.

We measured MALDI-TOF MS to support the FT-IR results and confirm that the ED60 oligosiloxane composition has a more condensed structure as compared to that of the other compositions. Fig. 3 presents the results of the MALDI-TOF MS of cycloaliphatic epoxy oligosiloxane resins synthesized with various silane precursor compositions. In the spectra, the structure of the cycloaliphatic epoxy oligosiloxane resins for all compositions is mainly tetramer, a reaction product of four identical silane precursors. In particular, the MALDI-TOF MS peaks of the ED60 oligosiloxane resin shift to peaks of species with high molecular weights compared to those of the ED40 oligosiloxane resin. This indicates that increased DPSD contents leads to the formation of highly condensed species in the resin.

Characteristics of hybrimer barrier coated film

We deposited the hybrimer barrier coating on a PET film *via* spin-coating. The optical properties, *i.e.*, the refractive index and transmittance, of the hybrimer barrier coated film were characterized by a prism coupler and UV/VIS/NIR spectroscopy with various compositions. Fig. 4 presents the refractive index of the hybrimer barrier coated films measured at a wavelength of 632.8 nm; the transmittance of the bare PET films with the hybrimer barrier coating were measured in the visible range of 400–800 nm. As the DPSD content was increased, the refractive index of the samples increased exponentially from 1.543 to 1.5704. From the Lorentz-Lorenz equation, the refractive index of the materials is directly proportional to the electronic polarizability and density. With an increase of the DPSD contents, more phenyl groups are introduced to the hybrimer barrier coated film and a more condensed inorganic network can be formed. Consequently, the refractive index of the hybrimer coated film increases exponentially.

It is well known that refractive index matching is an important factor in relation to the transmittance of composite materials.[21] When the refractive index of a multi-layered film is matched, the reflectance of light through the film can be minimized. Thus, a highly transparent multi-layered film can be fabricated. As can be seen in Fig. 5, the transmittance value of the bare PET film (n = 1.574 at 633 nm) is about 85%. Meanwhile, the average transmittance of hybrimer barrier coatings on the PET film is greater than 88% for all compositions, and the hybrimer barrier coating with a composition of ED60 on the PET film shows the highest transmittance value (>90%). In addition, the planarization of the rough PET surface with the hybrimer coating can reduce the reflectance. The high optical transmittance of the ED60 film attributed to refractive index matching between the hybrimer barrier coating and the PET film and the planarization of the rough PET surface.

The surface energy of the hybrimer barrier coated film was calculated by the Owens-Wendt's equation.[18] DI water and a diiodomethane (CH_2I_2) droplet (20μm) were deposited on the coated film surface using a micropipette, and a photograph of the water droplet was taken after 30 s at 25 °C using a goniometric camera for definition of the CA. Table 2 shows the contact-angle data of DI water and diiodomethane and the surface energy of the hybrimer barrier coated films. γ^d and γ^p denote the dispersion and polar components of the surface energy. The surface energy of the hybrimer barrier coating (γ) is the sum of γ^d and γ^p. The CA of DI water and diiodomethane of the hybrimer barrier coating varies from 72.4° to 82.0° and from 34.1° to 43.1° with growing DPSD contents, respectively. The surface energy of the

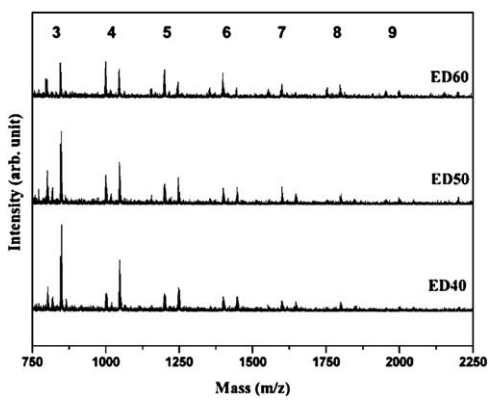

Fig. 3 MALDI-TOF MS spectra of the cycloaliphatic epoxy oligosiloxane resins with various compositions. Peaks corresponding to trimer, tetramer, pentamer, hexamer, heptamer, octamer, and nonamer are represented, respectively.

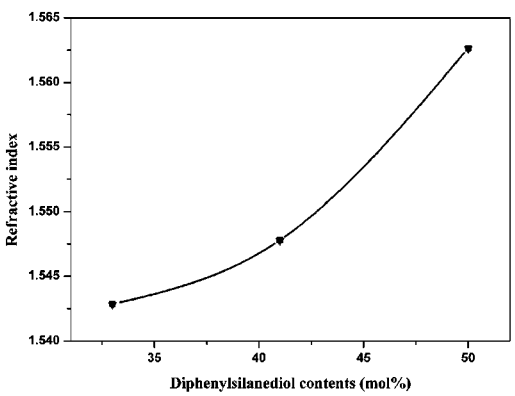

Fig. 4 Refractive indices of the hybrimer coated films with various DPSD contents.

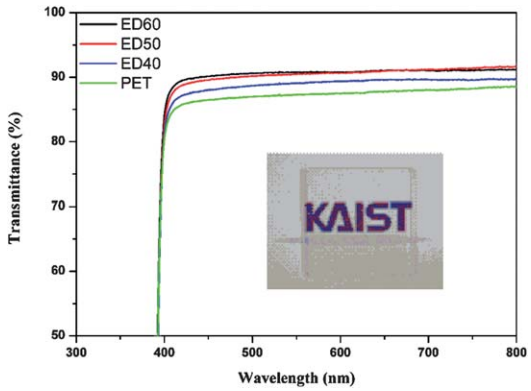

Fig. 5 Optical transmittance of the hybrimer barrier coatings with various compositions on a PET film and the bare PET film.

Table 2 Contact angle and surface energy of the hybrimer barrier coated films with different compositions

	Contact angle (°)		Surface energy/mJ m^{-2}		
Composition	DI water	CH_2I_2	γ^d	γ^p	γ
ED40	74.2	36.1	38.6	5.6	44.2
ED50	80.6	41.1	36.7	3.7	40.4
ED60	82.0	43.1	35.8	3.4	39.2

hybrimer barrier coating with ED40 composition, >45.4 mJ m^{-2}, is reduced down to >39.2 mJ m^{-2} with ED60 composition. With an increase of the DPSD content, more phenyl groups are introduced to the hybrimer barrier coated film. Consequently, the hydrophobicity of the hybrimer barrier coating increases with DPSD content.

A cross sectional image and the surface roughness of the hybrimer barrier coating were investigated by FE-SEM and AFM. In Fig. 6a are FE-SEM images of hybrimer barrier coatings applied with various spin rates. The thickness of the film was easily controlled from 2.2 μm to 8.1 μm with variation of the spin rate of the spin coater. The hybrimer barrier coating has a dense structure and a crack-free film is formed even in the case of 10 μm thickness. We also measured the surface roughness of the hybrimer barrier coating using AFM (Fig. 6b). The root mean square (rms) roughness of the hybrimer barrier coating is below 0.5 nm. This indicates that cycloaliphatic epoxy oligosiloxane has excellent coating and wetting behaviour and pinholes and defects are not formed during the coating step.

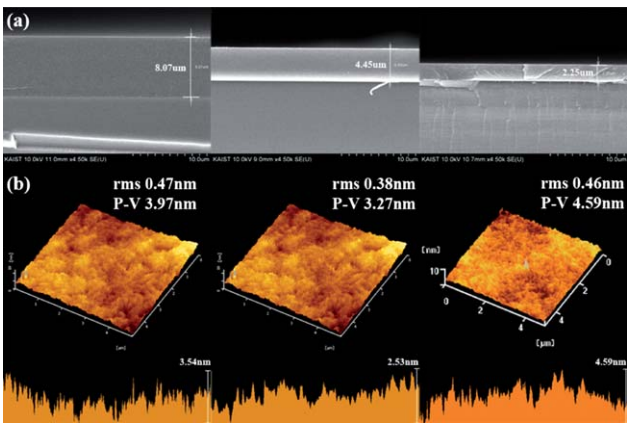

Fig. 6 FE-SEM images of the hybrimer barrier coating on a Si-wafer with various spin rates (a) 1000 rpm, 2000 rpm, and 5000 rpm, respectively and (b) 3-D and cross-sectional AFM images of the hybrimer barrier coating on a PET with various compositions.

Moisture barrier property of hybrimer barrier coated film

The moisture barrier property was characterized by the Ca degradation method. The amount of oxidative degradation in a thin Ca layer was monitored by measurement of resistance. The water vapor, permeating through the gas barrier on PET, oxidizes the Ca layer. This is reflected by decreasing current when a constant voltage is applied and can be monitored on a two point probe system. Fig. 7 shows the plot of the normalized resistivity (R_0/R) *versus* time of a single hybrimer barrier coating film at 25 °C and >90% RH with various compositions. The WVTR of samples with a 2 μm thick hybrimer barrier coating on a 100 μm thick PET film is 4.8 for the ED40 composition, 2.7 for the ED50 composition, and 2.5 g m^{-2} day^{-1} for the ED60 composition, respectively. The WVTR of PET film with 100 μm thickness is 24.4 g m^{-2} day^{-1}. These WVTR values were also confirmed by MOCON (MOCON PERMATRAN-W Model 3/33, USA)†. The experimental results of the Ca test and MOCON test agree well matched with each other. The permeability was easily calculated using an equation[22] below.

$$\frac{l_t}{P} = \frac{l_1}{P_1} + \frac{l_2}{P_2} + \frac{l_3}{P_3} + \ldots \frac{l_n}{P_n}$$

where P is the permeability of the composite, l_t is the total thickness, P_i is the permeability of layers 1, 2, 3, ….n and l_i is the thickness of layers 1, 2, 3, …n.

The permeability of the hybrimer barrier coating is improved from 1.45 to 0.68 g m^{-2} day^{-1} per mil (25.4 μm) with increment of DPSD contents. This result is attributed to minimized pathways for water molecules through barrier film with an increase of the DPSD contents, which provide a higher packing density, and lower surface energy equates with hydrophobic characteristics. In addition, hydroxyl groups, generated by the epoxy polymerization, can reduce the penetration of water molecules by

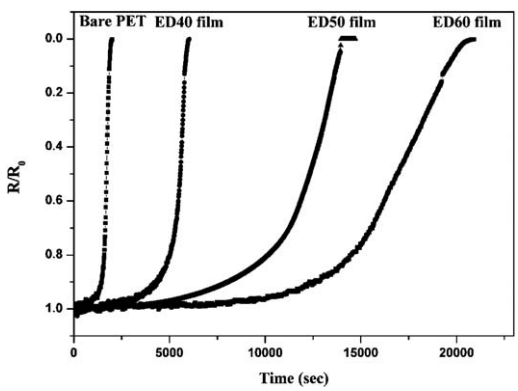

Fig. 7 Plots of the normalized resistivity (R_0/R) for Ca test *versus* time of a single hybrimer barrier coated film with various silane precursor compositions measured at 25 °C and 90% RH.

polar-polar interaction. Consequently, the hybrimer barrier coated film with ED60 composition shows the lowest permeability to water molecules.

Fig. 8 shows the OLED device luminescence and applied voltage against measuring time at 25 °C and >90% RH. We tested the hybrimer barrier coated film with an ED60 composition as a water vapor barrier for OLEDs. For comparison, we also measured the life-time of an un-capped and a PET encapsulated OLED device, respectively. All the devices were initially tested under an inert atmosphere prior to encapsulation of samples. There was little degradation of the encapsulated OLEDs at the initial stage. Applied voltage of 100 cd m^{-2} was from 4.5 V at the initial state to 4.65 V for the encapsulated OLEDs. We believe this degradation of encapsulated OLED devices originated from UV light exposure during polymerization of the epoxy sealant. The life-time of OLEDs was measured in a chamber that was maintained at 25 °C and >90% RH. We defined the life-time of OLED devices as the time when the luminescence and applied voltages are reduced to 50% of their initial values. The life-time of un-capped and PET encapsulated OLED devices was, 1.1 h and 2.8 h, respectively, under harsh conditions. From the results of the accelerated environmental test for thin-film encapsulation consisting of a hybrimer barrier coating on PET, the life-time of the encapsulated OLEDs is 11 h.

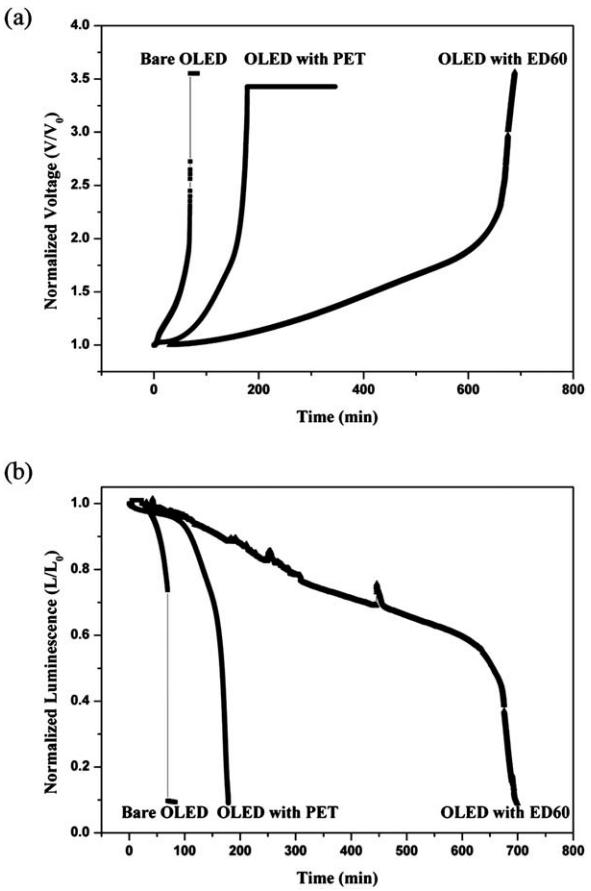

Fig. 8 Life time measurement of encapsulated OLEDs with bare PET and optimized hybrimer barrier coating film (ED60 composition). Normalized applied voltage (a) and normalized luminescence (b) *versus* time measured at 25 °C and 90% RH.

The life-time of the hybrimer barrier coated film encapsulated OLEDs was increased roughly 10-fold compared to that of an un-capped device and 4-fold compared to that of PET encapsulated devices. These results demonstrate that the hybrimer barrier coating has a water vapor barrier property and can be applied to organic electronics.

Conclusion

Cycloaliphatic epoxy oligosiloxane resins were synthesized by non-hydrolytic sol–gel condensation of DPSD and ECTS and their physical and chemical characteristics were investigated. The resins were polymerized by UV-induced polymerization to be used as an OLED encapsulant. The fabricated hybrimers have a highly dense structure without any defects. As the DPSD content of the hybrimers was increased, the higher packing density, transparency and lower surface energy were obtained. The permeability of the hybrimer barrier coated film to water vapor was measured by the Ca degradation test method. The hybrimer barrier coated film exhibits a low permeability value of 0.68 g m^{-2} day^{-1} per mil and OLEDs encapsulated using the hybrimer barrier coated film showed extended life time. Hybrimers can be effectively employed in barrier films such as organic electronics and flexible display substrates and provide enhanced barrier properties with high transparency.

Acknowledgements

This research was supported by Basic Science Research Program through the National Research Foundation of Korea (NRF) funded by the Ministry of Education, Science and Technology (No. R11-2007-045-03002-0). The authors gratefully thank the Korea Basic Science Institute for NMR spectra measurements.

References

1 H. Ito, W. Oka, H. Goto and H. Umeda, *Jpn. J. Appl. Phys.*, 2006, **45**, 4325.
2 J. –W. Park, Y. Kim, H. Lim, C. M. Bae, I. Kim, S. Ando and C. –S. Ha, *Mat. Res. Soc. Symp. Proc.*, 2004, 814.
3 K. R. Sarma, J. Roush, J. Schmidt, C. Chanley and S. Dodd, *Proc. of ASID '06*, 2006, 337.
4 H. Aziz, Z. Popovic, S. Xie, A. M. Hor, N. X. Hu, C. Tripp and G. Xu, *Appl. Phys. Lett.*, 1998, **72**, 756.
5 P. E. Burrows, V. Bulovic, S. R. Forrest, L. S. Saposhak, D. M. McCarty and M. E. Thompson, *Appl. Phys. Lett.*, 1994, **65**, 2922.
6 A. B. Cheang, M. A. Rothman, S. Y. Mao, R. H. Hewitt, M. S. Weaver, J. A. Silvernail, K. Rajan, M. Hack, J. J. Brown, X. Chu, L. Moro, T. Krajewski and N. Rutherford, *Appl. Phys. Lett.*, 1998, **72**, 756.
7 P. F. Carcia, R. S. Mclean, M. H. Reilly, M. D. Gronor, S. M. George and C. Tripp, *Appl. Phys. Lett.*, 1998, **72**, 756.
8 G. L. Graff, R. E. Williford and P. E. Burrows, *Appl. Phys. Lett.*, 2004, **96**, 1840.
9 J. S. Lewis and M. S. Weaver, *IEEE J. Sel. Top. Quantum Electron.*, 2004, **10**, 45.
10 D. Vangeneugden, S. Paulussen, O. Goossens, R. Rego and K. Rose, *Chem. Vap. Deposition*, 2005, **11**, 491.
11 R. Houbertz, J. Schulz, L. Fröhlich, G. Domann and M. Popall, *Mat. Res. Soc. Proc.*, 2003, 769.
12 Y. J. Eo, T. H. Lee, S. Y. Kim, J. K. Kang, Y. S. Han and B. S. Bae, *J. Polym. Sci., Part B: Polym. Phys.*, 2005, **43**(7), 827–836.
13 K. H. Jung and B. –S. Bae, *J. Appl. Polym. Sci.*, 2008, **108**, 3169–3176.
14 C. G. Choi and B.-S. Bae, *Synth. Met.*, 2009, **159**, 1288–1291.

15 T. H. Lee, J. H. Kim and B. –S. Bae, *J. Mater. Chem.*, 2006, **16**, 1657–1664.
16 R. Paetzold, A. Winnacker, D. Henseler, V. Cesari and K. Heuser, *Rev. Sci. Instrum.*, 2003, **74**, 5147.
17 M. S. Weaver, L. A. Michalski, K. Rajan, M. A. Rothman, J. A. Silvernail, P. E. Burrows, G. L. Graff, M. E. Gross, P. M. Martin, M. Hall, E. Mast, C. Bonham, W. Bennett and M. Zumhoff, *Appl. Phys. Lett.*, 2002, **14**, 2929.
18 D. K. Owens and R. C. Wendt, *J. Appl. Polym. Sci.*, 1969, **13**, 1741.
19 S. Sepeur, N. Kunze, B. Werner and H. Schmidt, *Thin Solid Films*, 1999, **351**, 216.
20 Z. Sassi, J. C. Bureau and A. Bakkali, *Vib. Spectrosc.*, 2002, **28**, 299.
21 I. Moreno, J. J. Araiza and M. A. Alejo, *Opt. Lett.*, 2005, **30**, 914.
22 W. E. Brown, C. R. Finch, A. Speigel, and J. H. Heckman, *Plastics in Food Packaging-Properties, Design and Fabrication*, Marcel Dekker, Inc, New York 1992.